

MODULATION-MODE ASSIGNMENT IN SVD-ASSISTED BROADBAND MIMO-BICM SCHEMES

Andreas Ahrens

Hochschule Wismar, University of Technology, Business and Design, Philipp-Müller-Straße 14, 23966 Wismar, Germany

César Benavente-Peces

Universidad Politécnica de Madrid, Ctra. Valencia. km. 7, 28031 Madrid, Spain

Keywords: Multiple-Input Multiple-Output (MIMO) System, Wireless Transmission, EXIT Charts, Singular-Value Decomposition, Bit-Interleaved Coded Modulation (BICM), Iterative Decoding, Bit-Interleaved Coded Irregular Modulation (BICIM), Spatial Division Multiplexing (SDM).

Abstract: In this contribution we jointly optimize the number of activated MIMO layers and the number of bits per symbol under the constraint of a given fixed data throughput and integrity. In analogy to bit-interleaved coded irregular modulation, we introduce a Broadband MIMO-BICM scheme, where different signal constellations and mappings were used within a single codeword. Extrinsic information transfer (EXIT) charts are used for analyzing and optimizing the convergence behaviour of the iterative demapping and decoding. Our results show that in order to achieve the best bit-error rate, not necessarily all MIMO layers have to be activated.

1 INTRODUCTION

Iterative demapping and decoding aided bit-interleaved coded modulation (BICM-ID) was designed for bandwidth efficient transmission over fading channels (Caire et al., 1998; Chindapol, 2001). The BICM philosophy has been extended by using different signal constellations and bit-to-symbol mapping arrangements within a single codeword, leading to the concept of bit-interleaved coded irregular modulation (BICIM) schemes, offering an improved link adaptation capability and an increased design freedom (Schreckenbach and Bauch, 2006). Since the capacity of multiple-input multiple-output (MIMO) systems increases linearly with the minimum number of antennas at both, the transmitter as well as the receiver side, MIMO-BICM schemes have attracted substantial attention (McKay and Collings, 2005; Mueller-Weinfurter, 2002) and can be considered as an essential part of increasing both the achievable capacity and integrity of future generations of wireless systems (Kühn, 2006; Zheng and Tse, 2003). However, their parameters have to be carefully optimized, especially in conjunction with adaptive modulation (Zhou et al., 2005). In general, non-frequency selective MIMO links have attracted a

lot of research and have reached a state of maturity (Kühn, 2006; Ahrens and Lange, 2008). By contrast, frequency selective MIMO links require substantial further research, where spatio-temporal vector coding (STVC) introduced by RALEIGH seems to be an appropriate candidate for broadband transmission channels (Raleigh and Cioffi, 1998; Raleigh and Jones, 1999). In general, the choice of the number of bits per symbol and the number of activated MIMO layers combined with powerful error correcting codes offer a certain degree of design freedom, which substantially affects the performance of MIMO systems. In addition to bit loading algorithms, in this contribution the benefits of channel coding are also investigated. The proposed iterative decoder structures employ symbol-by-symbol soft-output decoding based on the Bahl-Cocke-Jelinek-Raviv (BCJR) algorithm and are analyzed under the constraint of a fixed data throughput (Bahl et al., 1974). Against this background, the novel contribution of this paper is that we jointly optimize the number of activated MIMO layers and the number of bits per symbol combined with powerful error correcting codes under the constraint of a given fixed data throughput and integrity. Since the "design-space" is large, a two-stage optimization technique is

considered. Firstly, the uncoded spatial division multiplexing (SDM) broadband MIMO scheme is analyzed, investigating the allocation of both the number of bits per modulated symbol and the number of activated MIMO layers at a fixed data rate. Secondly, the optimized uncoded system is extended by incorporating bit-interleaved coded modulation using iterative detection (BICM-ID), whereby both the uncoded as well as the coded systems are required to support the same user data rate within the same bandwidth.

This contribution is organized as follows: Section 2 introduces our system model, while the proposed uncoded solutions are discussed in Section 3. In Section 4 the channel encoded MIMO system is introduced, while the computation of the EXIT transfer function is presented in Section 5. The associated performance results are presented and interpreted in Section 6. Finally, Section 7 provides our concluding remarks.

2 SYSTEM MODEL

When considering a frequency selective SDM MIMO link, composed of n_T transmit and n_R receive antennas, the block-oriented system is modelled by

$$\mathbf{u} = \mathbf{H} \cdot \mathbf{c} + \mathbf{w} \quad (1)$$

In (1), \mathbf{c} is the $(N_T \times 1)$ transmitted signal vector containing the complex input symbols transmitted over n_T transmit antennas in K consecutive time slots, i. e., $N_T = K n_T$. This vector can be decomposed into n_T antenna-specific signal vectors \mathbf{c}_μ according to

$$\mathbf{c} = (\mathbf{c}_1^T, \dots, \mathbf{c}_\mu^T, \dots, \mathbf{c}_{n_T}^T)^T \quad (2)$$

In (2), the $(K \times 1)$ antenna-specific signal vector \mathbf{c}_μ transmitted by the transmit antenna μ (with $\mu = 1, \dots, n_T$) is modelled by

$$\mathbf{c}_\mu = (c_{1\mu}, \dots, c_{k\mu}, \dots, c_{K\mu})^T \quad (3)$$

The $(N_R \times 1)$ received signal vector \mathbf{u} , defined in (1), can again be decomposed into n_R antenna-specific signal vectors \mathbf{u}_v (with $v = 1, \dots, n_R$) of the length $K + L_c$, i. e., $N_R = (K + L_c) n_R$, and results in

$$\mathbf{u} = (\mathbf{u}_1^T, \dots, \mathbf{u}_v^T, \dots, \mathbf{u}_{n_R}^T)^T \quad (4)$$

By taking the $(L_c + 1)$ non-zero elements of the resulting symbol rate sampled overall channel impulse response between the μ th transmit and v th receive antenna into account, the antenna-specific received vector \mathbf{u}_v has to be extended by L_c elements, compared to

the transmitted antenna-specific signal vector \mathbf{c}_μ defined in (3). The $((K + L_c) \times 1)$ signal vector \mathbf{u}_v received by the antenna v (with $v = 1, \dots, n_R$) can be constructed, including the extension through the multipath propagation, as follows

$$\mathbf{u}_v = (u_{1v}, u_{2v}, \dots, u_{(K+L_c)v})^T \quad (5)$$

Similarly, in (1) the $(N_R \times 1)$ noise vector \mathbf{w} results in

$$\mathbf{w} = (\mathbf{w}_1^T, \dots, \mathbf{w}_v^T, \dots, \mathbf{w}_{n_R}^T)^T \quad (6)$$

The vector \mathbf{w} of the additive, white Gaussian noise (AWGN) is assumed to have a variance of U_R^2 for both the real and imaginary parts and can still be decomposed into n_R antenna-specific signal vectors \mathbf{w}_v (with $v = 1, \dots, n_R$) according to

$$\mathbf{w}_v = (w_{1v}, w_{2v}, \dots, w_{(K+L_c)v})^T \quad (7)$$

Finally, the $(N_R \times N_T)$ system matrix \mathbf{H} of the block-oriented system model, introduced in (1), results in

$$\mathbf{H} = \begin{bmatrix} \mathbf{H}_{11} & \dots & \mathbf{H}_{1n_T} \\ \vdots & \ddots & \vdots \\ \mathbf{H}_{n_R1} & \dots & \mathbf{H}_{n_Rn_T} \end{bmatrix}, \quad (8)$$

and consists of $n_R n_T$ single-input single-output (SISO) channel matrices $\mathbf{H}_{v\mu}$ (with $v = 1, \dots, n_R$ and $\mu = 1, \dots, n_T$). The system description, called spatio-temporal vector coding (STVC), was introduced by RALEIGH. Every of these matrices $\mathbf{H}_{v\mu}$ with the dimension $((K + L_c) \times K)$ describes the influence of the channel from transmit antenna μ to receive antenna v including transmit and receive filtering. The channel convolution matrix $\mathbf{H}_{v\mu}$ between the μ th transmit and v th receive antenna is obtained by taking the $(L_c + 1)$ non-zero elements of resulting symbol rate sampled overall impulse response into account and results in:

$$\mathbf{H}_{v\mu} = \begin{bmatrix} h_0 & 0 & 0 & \dots & 0 \\ h_1 & h_0 & 0 & \dots & \vdots \\ h_2 & h_1 & h_0 & \dots & 0 \\ \vdots & h_2 & h_1 & \dots & h_0 \\ h_{L_c} & \vdots & h_2 & \dots & h_1 \\ 0 & h_{L_c} & \vdots & \dots & h_2 \\ 0 & 0 & h_{L_c} & \dots & \vdots \\ 0 & 0 & 0 & \dots & h_{L_c} \end{bmatrix} \quad (9)$$

Throughout this paper, it is assumed that the $(L_c + 1)$ channel coefficients, between the μ th transmit and v th receive antenna have the same averaged power and undergo a Rayleigh distribution. Furthermore, a block fading channel model is applied, i. e., the channel is

assumed to be time invariant for the duration of one SDM MIMO data vector.

The interference between the different antenna's data streams, which is introduced by the off-diagonal elements of the channel matrix \mathbf{H} , requires appropriate signal processing strategies. A popular technique is based on the singular-value decomposition (SVD) (Haykin, 2002) of the system matrix \mathbf{H} , which can be written as $\mathbf{H} = \mathbf{S} \cdot \mathbf{V} \cdot \mathbf{D}^H$, where \mathbf{S} and \mathbf{D}^H are unitary matrices and \mathbf{V} is a real-valued diagonal matrix of the positive square roots of the eigenvalues of the matrix $\mathbf{H}^H \mathbf{H}$ sorted in descending order¹. The SDM MIMO data vector \mathbf{c} is now multiplied by the matrix \mathbf{D} before transmission. In turn, the receiver multiplies the received vector \mathbf{u} by the matrix \mathbf{S}^H . Thereby neither the transmit power nor the noise power is enhanced. The overall transmission relationship is defined as

$$\mathbf{y} = \mathbf{S}^H (\mathbf{H} \cdot \mathbf{D} \cdot \mathbf{c} + \mathbf{w}) = \mathbf{V} \cdot \mathbf{c} + \tilde{\mathbf{w}}. \quad (10)$$

As a consequence of the processing in (10), the channel matrix \mathbf{H} is transformed into independent, non-interfering layers having unequal gains.

3 QUALITY CRITERIA

In general, the quality of data transmission can be informally assessed by using the signal-to-noise ratio (SNR) at the detector's input defined by the half vertical eye opening and the noise power per quadrature component according to

$$\rho = \frac{(\text{Half vertical eye opening})^2}{\text{Noise Power}} = \frac{(U_A)^2}{(U_R)^2}, \quad (11)$$

which is often used as a quality parameter (Ahrens and Lange, 2008). The relationship between the signal-to-noise ratio $\rho = U_A^2/U_R^2$ and the bit-error probability evaluated for AWGN channels and M -ary Quadrature Amplitude Modulation (QAM) is given by (Proakis, 2000)

$$P_{\text{BER}} = \frac{2}{\log_2(M)} \left(1 - \frac{1}{\sqrt{M}}\right) \text{erfc} \left(\sqrt{\frac{\rho}{2}} \right). \quad (12)$$

When applying the proposed system structure, the SVD-based equalization leads to different eye openings per activated MIMO layer ℓ (with $\ell = 1, 2, \dots, L$) at the time k (with $k = 1, 2, \dots, K$) within the SDM MIMO signal vector according to

$$U_A^{(\ell,k)} = \sqrt{\xi_{\ell,k}} \cdot U_{s\ell}, \quad (13)$$

¹The transpose and conjugate transpose (Hermitian) of \mathbf{D} are denoted by \mathbf{D}^T and \mathbf{D}^H , respectively.

where $U_{s\ell}$ denotes the half-level transmit amplitude assuming M_ℓ -ary QAM and $\sqrt{\xi_{\ell,k}}$ represents the corresponding positive square roots of the eigenvalues of the matrix $\mathbf{H}^H \mathbf{H}$. Together with the noise power per quadrature component, the SNR per MIMO layer ℓ at the time k becomes

$$\rho^{(\ell,k)} = \frac{(U_A^{(\ell,k)})^2}{U_R^2} = \xi_{\ell,k} \frac{(U_{s\ell})^2}{U_R^2}. \quad (14)$$

Using the parallel transmission over $L \leq \min(n_T, n_R)$ MIMO layers, the overall mean transmit power becomes $P_s = \sum_{\ell=1}^L P_{s\ell}$, where the number of readily separable layers² is limited by $\min(n_T, n_R)$. Considering QAM constellations, the average transmit power $P_{s\ell}$ per MIMO layer ℓ may be expressed as (Proakis, 2000)

$$P_{s\ell} = \frac{2}{3} U_{s\ell}^2 (M_\ell - 1). \quad (15)$$

Combining (14) and (15), the layer-specific SNR at the time k results in

$$\rho^{(\ell,k)} = \xi_{\ell,k} \frac{3}{2(M_\ell - 1)} \frac{P_{s\ell}}{U_R^2}. \quad (16)$$

In order to transmit at a fixed data rate while maintaining the best possible integrity, i. e., bit-error rate, an appropriate number of MIMO layers has to be used, which depends on the specific transmission mode, as detailed in Table 1. In general, the BER per SDM MIMO data vector is dominated by the specific transmission modes and the characteristics of the singular values, resulting in different BERs for the different QAM configurations in Table 1. An optimized adaptive scheme would now use the particular transmission modes, e. g., by using bit auction procedures (Wong et al., 1999), that results in the lowest BER for each SDM MIMO data vector. This would lead to different transmission modes per SDM MIMO data vector and a high signaling overhead would result. However, in order to avoid any signalling overhead, fixed transmission modes are used in this contribution regardless of the channel quality. The MIMO layer specific bit-error probability at the time k after SVD is given by (Ahrens and Lange, 2008)

$$P_{\text{BER}}^{(\ell,k)} = \frac{2 \left(1 - \frac{1}{\sqrt{M_\ell}}\right)}{\log_2(M_\ell)} \text{erfc} \left(\sqrt{\frac{\rho^{(\ell,k)}}{2}} \right). \quad (17)$$

The resulting average bit-error probability at the time k assuming different QAM constellation sizes per ac-

²It is worth noting that with the aid of powerful non-linear near Maximum Likelihood (ML) sphere decoders it is possible to separate $n_R > n_T$ number of layers (Hanzo and Keller, 2006).

Table 1: Investigated transmission modes.

throughput	layer 1	layer 2	layer 3	layer 4
8 bit/s/Hz	256	0	0	0
8 bit/s/Hz	64	4	0	0
8 bit/s/Hz	16	16	0	0
8 bit/s/Hz	16	4	4	0
8 bit/s/Hz	4	4	4	4

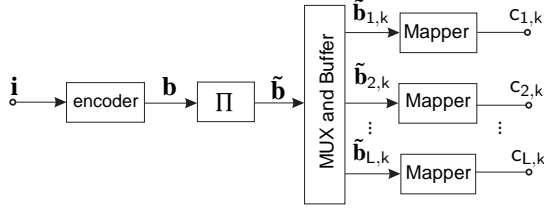


Figure 1: The channel-encoded MIMO transmitter's structure.

tivated MIMO layer is given by

$$P_{\text{BER}}^{(k)} = \frac{1}{\sum_{v=1}^L \log_2(M_v)} \sum_{\ell=1}^L \log_2(M_\ell) P_{\text{BER}}^{(\ell,k)}. \quad (18)$$

Taking K consecutive time slots into account, needed to transmit the SDM MIMO data vector, the aggregate bit-error probability per SDM MIMO data vector yields

$$P_{\text{BER block}} = \frac{1}{K} \sum_{k=1}^K P_{\text{BER}}^{(k)}. \quad (19)$$

When considering time-variant channel conditions, rather than an AWGN channel, the BER can be derived by considering the different transmission block SNRs. Assuming that the transmit power is uniformly distributed over the number of activated MIMO layers, i. e., $P_{s\ell} = P_s/L$, the half-level transmit amplitude $U_{s\ell}$ per activated MIMO layer results in

$$U_{s\ell} = \sqrt{\frac{3P_s}{2L(M_\ell - 1)}}. \quad (20)$$

Finally, the layer-specific signal-to-noise ratio at the time k , defined in (14), results together with (20) in

$$\rho^{(\ell,k)} = \xi_{\ell,k} \frac{3}{2L(M_\ell - 1)} \frac{P_s}{U_R^2} = \xi_{\ell,k} \frac{3}{L(M_\ell - 1)} \frac{E_s}{N_0}, \quad (21)$$

with

$$\frac{P_s}{U_R^2} = \frac{E_s}{N_0/2}. \quad (22)$$

4 CODED MIMO SYSTEM

The transmitter structure including channel coding is depicted in Figure 1. The encoder employs a

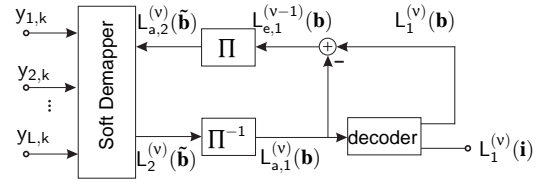


Figure 2: Iterative demodulator structure.

half-rate nonrecursive, non-systematic (NSC) convolutional code using the generator polynomials (7, 5) in octal notation. The uncoded information is organized in blocks of N_i bits, consisting of at least 3000 bits, depending on the specific QAM constellation used. Each data block \mathbf{i} is encoded and results in the block \mathbf{b} consisting of $N_b = 2N_i + 4$ encoded bits, including 2 termination bits. The encoded bits are interleaved using a random interleaver and stored in the vector $\tilde{\mathbf{b}}$. The encoded and interleaved bits are then mapped to the MIMO layers. The task of the multiplexer and buffer block of Figure 1 is to divide the vector of encoded and interleaved information bits $\tilde{\mathbf{b}}$ into subvectors $(\tilde{\mathbf{b}}_{1,k}, \tilde{\mathbf{b}}_{2,k}, \dots, \tilde{\mathbf{b}}_{L,k})$, each consisting of 8 bits according to the chosen transmission mode (Table 1). The individual binary data vectors $\tilde{\mathbf{b}}_{\ell,k}$ are then mapped to the QAM symbols $c_{\ell,k}$ according to the specific mapper used. The iterative demodulator structure is shown in Figure 2 (Ahrens et al., 2008). A detailed structure of the soft demapper structure is portrayed in Figure 3. When using the iteration index v , the first iteration of $v = 1$ commences with the soft-demapper delivering the N_b log-likelihood ratios (LLRs) $L_2^{(v=1)}(\tilde{\mathbf{b}})$ of the encoded and interleaved information bits, whose de-interleaved version $L_{a,1}^{(v=1)}(\mathbf{b})$ represents the input of the convolutional decoder as depicted in Figure 2 (Bahl et al., 1974; Kühn, 2006). This channel decoder provides the estimates $L_1^{(v=1)}(\mathbf{i})$ of the original uncoded information bits as well as the LLRs of the N_b NSC-encoded bits in the form of

$$L_1^{(v=1)}(\mathbf{b}) = L_{a,1}^{(v=1)}(\mathbf{b}) + L_{e,1}^{(v=1)}(\mathbf{b}). \quad (23)$$

As seen in Figure 2 and (23), the LLRs of the NSC-encoded bits consist of the receiver's input signal itself plus the extrinsic information $L_{e,1}^{(v=1)}(\mathbf{b})$, which is generated by subtracting $L_{a,1}^{(v=1)}(\mathbf{b})$ from $L_1^{(v=1)}(\mathbf{b})$. The appropriately ordered, i. e. interleaved extrinsic LLRs are fed back as *a priori* information $L_{a,2}^{(v=2)}(\tilde{\mathbf{b}})$ to the soft demapper of Figure 2 for the second iteration. Following the detailed structure of the soft-demapper in Figure 3, the N_b LLRs $L_2^{(v)}(\tilde{\mathbf{b}})$ are composed of the subvectors $(L_2^{(v)}(\tilde{\mathbf{b}}_{1,k}), L_2^{(v)}(\tilde{\mathbf{b}}_{2,k}), \dots, L_2^{(v)}(\tilde{\mathbf{b}}_{L,k}))$, each consist-

ing of 8 elements according to the chosen transmission mode (Table 1). Each vector $L_2^{(v)}(\tilde{\mathbf{b}}_{\ell,k})$ is generated by the soft demapper from the MIMO channel's output $y_{\ell,k}$ and the *a-priori* information $L_{a,2}^{(v)}(\tilde{\mathbf{b}}_{\ell,k})$ provided by the channel decoder. After the first iteration, this *a-priori* information emerges from the N_b LLRs $L_{a,2}^{(v)}(\tilde{\mathbf{b}})$, which are again decomposed into the subvectors $(L_{a,2}^{(v)}(\tilde{\mathbf{b}}_{1,k}), L_{a,2}^{(v)}(\tilde{\mathbf{b}}_{2,k}), \dots, L_{a,2}^{(v)}(\tilde{\mathbf{b}}_{L,k}))$, each consisting of 8 elements.

5 EXIT TRANSFER FUNCTION

Random variables (r.v.s) are denoted with capital letters and their corresponding realizations with lower case letters. Sequences of random variables and realizations are indicated by boldface italic letters (as \mathbf{B} or \mathbf{b}). Furthermore, boldface roman letters denote vectors (as \mathbf{B} or \mathbf{b}). The time instant is denoted with k and the layer with ℓ . The transmitted data sequence \mathbf{B} is multiplexed onto the different used MIMO layers ℓ and results in the MIMO layer specific sequence \mathbf{B}_ℓ with $\ell = 1, 2, \dots, L$. The stationary binary input sequence $\mathbf{B}_\ell = [B_{\ell,1}, B_{\ell,2}, \dots, B_{\ell,k}, \dots]$ consists of r.v.s $B_{\ell,k}$, where the corresponding realizations $b_{\ell,k}$ have an index length of 1 bit and are taken from a finite alphabet $\mathcal{B} = \{0, 1\}$. The mapper output sequence $\mathbf{C}_\ell = [C_{\ell,1}, C_{\ell,2}, \dots, C_{\ell,k}, \dots]$ on the ℓ -th layer consists of r.v.s $C_{\ell,k}$, where the corresponding realizations $c_{\ell,k}$ have an index length of $\log_2(M_\ell)$ bits and are taken from a finite alphabet $\mathcal{C} = \{0, 1, \dots, M_\ell - 1\}$. The symbols $c_{\ell,k}$ are transmitted over independent channels resulting in the received values $y_{\ell,k}$. The *a priori* channel, as depicted in Figure 4, models the *a priori* information used at the soft demapper. The sequence $\mathbf{A}_\ell = [A_{\ell,1}, A_{\ell,2}, \dots, A_{\ell,k}, \dots]$ with the corresponding realizations $a_{\ell,k}$ contains the *a priori* LLR information passed to the demapper. EXIT charts visualize

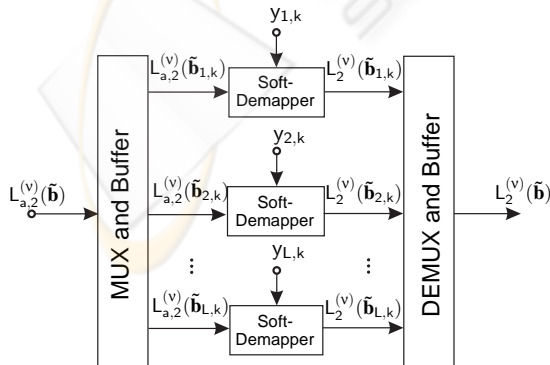


Figure 3: Detailed soft demapper demodulator structure.

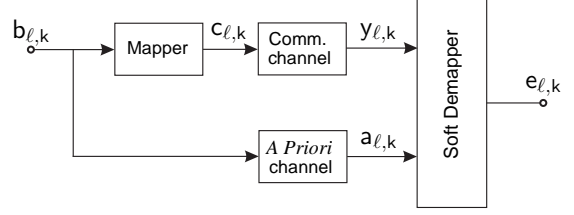


Figure 4: Transmission model analyzing the ℓ -th MIMO layer.

the input/output characteristics of the soft demapper and the decoder in terms of a mutual information transfer between the data sequence \mathbf{B}_ℓ and the sequence \mathbf{A}_ℓ of the *a priori* LLR information at the input of the soft demapper, as well as between \mathbf{B}_ℓ and the sequence \mathbf{E}_ℓ of the extrinsic LLR at the output, respectively. Denoting the mutual information between two r.v.s X and Y as $I(X; Y)$ we may define for a given sequence \mathbf{B}_ℓ the quantities $I_{\ell,A} = I(\mathbf{A}_\ell; \mathbf{B}_\ell)$ as well as $I_{\ell,E} = I(\mathbf{E}_\ell; \mathbf{B}_\ell)$. Herein, $I_{\ell,A}$ represents the average *a priori* information and $I_{\ell,E}$ the average extrinsic information, respectively (Ahrens et al., 2008). The transfer characteristic T of the soft demapper is given by $I_{\ell,E} = T(I_{\ell,A}, \rho)$, where ρ represents the SNR of the communication channel. Analyzing the outer decoder in a serially concatenated scheme T does not depend on ρ . An EXIT chart is now obtained by plotting the transfer characteristics T for both the demapper and the decoder within a single diagram, where the axes have to be swapped for one of the constituent decoders (Brink, 2001) (normally the outer one for serial concatenation).

Analyzing the layer specific characteristics, a MIMO-layer specific parameter $\alpha^{(\ell)}$ can be defined according to

$$\alpha^{(\ell)} = \frac{\log_2(M_\ell)}{R}, \quad (24)$$

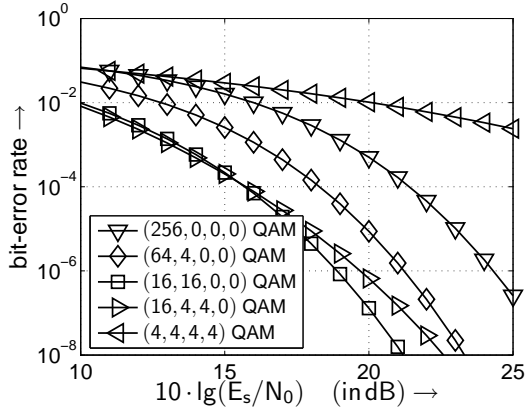
describing the fraction of the data sequence \mathbf{B} that is transmitted over the ℓ th layer, i. e. \mathbf{B}_ℓ (Ahrens et al., 2008). Therein, the parameter R describes the number of transmitted bits per time interval including all L MIMO layers and results in $R = \sum_{\ell=1}^L \log_2(M_\ell)$. Hence, the mutual information for a given sequence \mathbf{B} and the extrinsic LLR \mathbf{E} at the output is obtained by

$$I(\mathbf{E}; \mathbf{B}) = \sum_{\ell=1}^L \alpha^{(\ell)} I(\mathbf{E}_\ell; \mathbf{B}_\ell). \quad (25)$$

The MIMO layer specific extrinsic LLR sequences \mathbf{E}_ℓ are multiplexed onto the sequence \mathbf{E} , which lead to the outer decoder (Ahrens et al., 2008). Beneficial values of $\alpha^{(\ell)}$ may be chosen by ensuring that there is an open EXIT tunnel between the soft demapper transfer characteristic and the decoder transfer

Table 2: Transmission modes and corresponding $\alpha^{(\ell)}$.

	$M_1, \alpha^{(1)}$	$M_2, \alpha^{(2)}$	$M_3, \alpha^{(3)}$	$M_4, \alpha^{(4)}$
8 bit/s/Hz	256, 1	0, 0	0, 0	0, 0
8 bit/s/Hz	64, 3/4	4, 1/4	0, 0	0, 0
8 bit/s/Hz	16, 1/2	16, 1/2	0, 0	0, 0
8 bit/s/Hz	16, 1/2	4, 1/4	4, 1/4	0, 0
8 bit/s/Hz	4, 1/4	4, 1/4	4, 1/4	4, 1/4

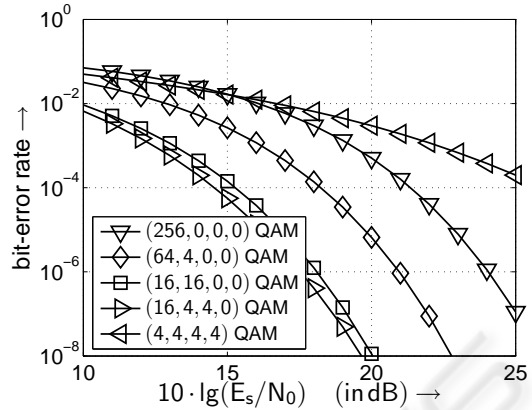

 Figure 5: BER when using the transmission modes introduced in Table 1 and transmitting 8 bit/s/Hz over frequency selective channels with $L_c = 1$.

characteristic at a given E_s/N_0 value that is close to the channel capacity bound. Analyzing the transmission modes in Table 1, the resulting values of $\alpha^{(\ell)}$ are shown in Table 2.

6 RESULTS

In this contribution fixed transmission modes are used regardless of the channel quality. Assuming predefined transmission modes, a fixed data rate can be guaranteed. The obtained uncoded BER curves are depicted in Figure 5 and 6 for the different QAM constellation sizes and MIMO configurations of Table 1, when transmitting at a bandwidth efficiency of 8 bit/s/Hz³. Assuming a uniform distribution of the transmit power over the number of activated MIMO layers, it turns out that not all MIMO layers have to be activated in order to achieve the best BERs. More explicitly, our goal is to find that specific combination of the QAM mode and the number of MIMO layers, which gives the best possible BER performance at a

³The expression $\lg(\cdot)$ is considered to be the short form of $\log_{10}(\cdot)$.


 Figure 6: BER when using the transmission modes introduced in Table 1 and transmitting 8 bit/s/Hz over frequency selective channels with $L_c = 4$.

given fixed bit/s/Hz bandwidth efficiency. However, the lowest BERs can only be achieved by using bit auction procedures leading to a high signalling overhead. Analyzing the probability of choosing specific transmission modes by using optimal bitloading as illustrated in (Ahrens and Benavente-Peces, 2009) it turns out that at moderate SNR only an appropriate number of MIMO layers have to be activated, e.g., the (16, 4, 4, 0) QAM configuration.

Using the half-rate constraint-length $K_{cl} = 3$ NSC code, the BER performance is analyzed for an effective user throughput of 4 bit/s/Hz. The BER investigations using the NSC code are based on the best uncoded schemes of Table 1. The information word length is 3000 bits and a random interleaver is applied. In addition to the number of bits per symbol and the number of activated MIMO layers, the achievable performance of the iterative decoder is substantially affected by the specific mapping of the bits to both the QAM symbols as well as to the MIMO layers.

While the employment of the classic Gray-mapping is appropriate in the absence of *a priori* information, the availability of *a priori* information in iterative receivers requires an exhaustive search for finding the best non-Gray – synonymously also referred to as anti-Gray – mapping scheme (Chindapol, 2001). A mapping scheme optimized for perfect *a priori* information has usually a poor performance, when there is no *a priori* information. However, when applying iterative demapping and decoding, large gains can be achieved as long as the reliability of the *a priori* information increases with the number of iterations.

Analyzing the number of activated MIMO layers, the soft-demapper transfer characteristics are depicted in Figure 7 and 8 using anti-Gray mapping on all acti-

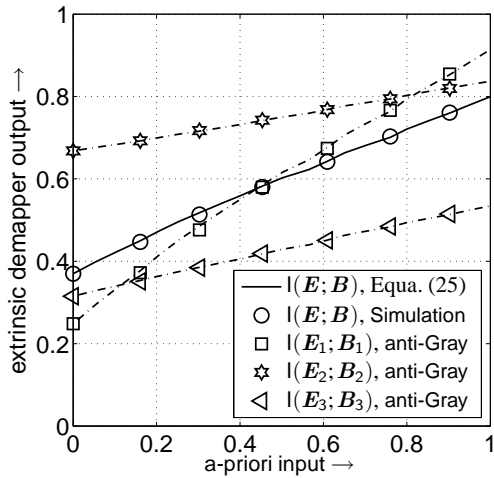


Figure 7: Layer-specific transfer characteristic when using anti-Gray mapping and the (16,4,4,0) transmission mode over frequency-selective MIMO links ($10 \log_{10}(E_s/N_0) = 2$ dB, $L_c = 1$).

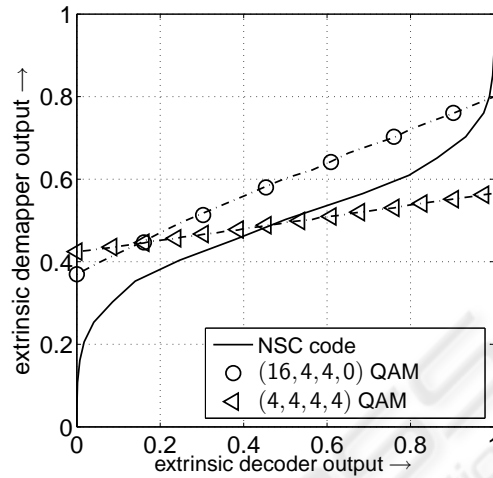


Figure 9: EXIT chart for an effective throughput of 4 bit/s/Hz when using anti-Gray mapping on all activated MIMO layers ($10 \log_{10}(E_s/N_0) = 2$ dB and $L_c = 1$) and the half-rate NSC code with the generator polynomials of (7,5) in octal notation.

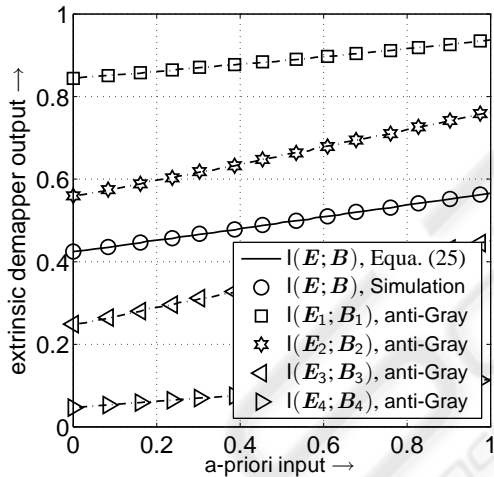


Figure 8: Layer-specific transfer characteristic when using anti-Gray mapping and the (4,4,4,4) transmission mode over frequency-selective MIMO links ($10 \log_{10}(E_s/N_0) = 2$ dB, $L_c = 1$).

activated MIMO layers. Assuming predefined QAM constellation sizes, the entire soft demapper transfer characteristic is well predictable by combining the single MIMO layer transfer characteristics using the parameter $\alpha^{(\ell)}$. Using predefined QAM constellation sizes and the corresponding $\alpha^{(\ell)}$, the resulting EXIT chart curve is depicted in Figure 9. In order to match the soft demapper transfer characteristic properly to the decoder transfer characteristic, a joint optimization of the number of activated MIMO layers as well as the number of bit per symbol has been carried out. Our results suggest that not all MIMO layers have to be

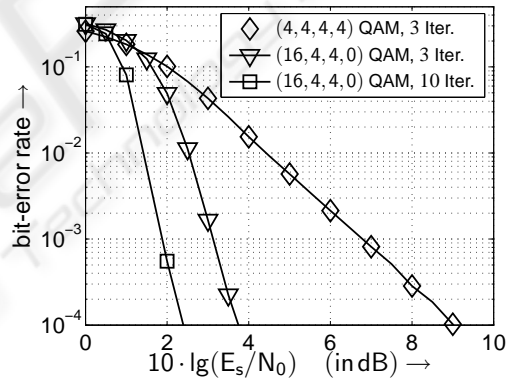


Figure 10: BER for an effective user throughput of 4 bit/s/Hz ($L_c = 1$) and anti-Gray mapping in combination with different transmission modes and the half-rate NSC code with the generator polynomials of (7,5) in octal notation.

activated in order to shape the soft demapper transfer characteristic properly. The best uncoded solutions seems also to be useful in the coded scenario. The corresponding BER curves are shown in Figure 10 and confirm the EXIT charts results. In order to guarantee an efficient information exchange between the soft-demapper and the decoder, i. e., an open EXIT tunnel, only an appropriate number of MIMO layers has to be activated. Using all MIMO layers for the data transmission, the information exchange between the soft-demapper and the decoder stops relatively early, as illustrated by the EXIT chart results in Figure 9, and significant enhancements in the BER performance can't be achieved any longer by increasing

the number of iterations at low SNR. As demonstrated along this work, it is showed that an appropriate number of MIMO layers seems to be a promising solution for minimizing the overall BER characteristic.

7 CONCLUSIONS

The choice of the number of bits per symbol and the number of MIMO layers combined with error correcting codes substantially affects the performance of a MIMO system. Analyzing the uncoded system, it turns out that not all MIMO layers have to be activated in order to achieve the best BERs. Considering the coded system, the choice of the mapping strategies combined with the appropriate number of activated MIMO layers and transmitted bits per symbol offers a certain degree of design freedom, which substantially affects the performance of MIMO systems. Here, using an appropriate number of MIMO layers for the data transmission seems to be a promising solution for minimizing the overall BER characteristic.

REFERENCES

- Ahrens, A. and Benavente-Peces, C. (2009). Modulation-Mode and Power Assignment in SVD-assisted Broadband MIMO Systems. In *International Conference on Wireless Information Networks and Systems (WINSYS)*, Milan (Italy).
- Ahrens, A. and Lange, C. (2008). Modulation-Mode and Power Assignment in SVD-equalized MIMO Systems. *Facta Universitatis (Series Electronics and Energetics)*, 21(2):167–181.
- Ahrens, A., Ng, S. X., Kühn, V., and Hanzo, L. (2008). Modulation-Mode Assignment for SVD-Aided and BICM-Assisted Spatial Division Multiplexing. *Physical Communications (PHYCOM)*, 1(1):60–66.
- Bahl, L. R., Cocke, J., Jelinek, F., and Raviv, J. (1974). Optimal Decoding of Linear Codes for Minimizing Symbol Error Rate. *IEEE Transactions on Information Theory*, 20(3):284–287.
- Brink, S. t. (2001). Convergence Behavior of Iteratively Decoded Parallel Concatenated Codes. *IEEE Transactions on Communications*, 49(10):1727–1737.
- Caire, G., Taricco, G., and Biglieri, E. (1998). Bit-Interleaved Coded Modulation. *IEEE Transactions on Information Theory*, 44(3):927–946.
- Chindapol, A. Ritcey, J. A. (2001). Design, Analysis, and Performance Evaluation for BICM-ID with square QAM Constellations in Rayleigh Fading Channels. *IEEE Journal on Selected Areas in Communications*, 19(5):944–957.
- Hanzo, L. and Keller, T. (2006). *OFDM and MC-CDMA*. Wiley, New York.
- Haykin, S. S. (2002). *Adaptive Filter Theory*. Prentice Hall, New Jersey.
- Kühn, V. (2006). *Wireless Communications over MIMO Channels – Applications to CDMA and Multiple Antenna Systems*. Wiley, Chichester.
- McKay, M. R. and Collings, I. B. (2005). Capacity and Performance of MIMO-BICM with Zero-Forcing Receivers. *IEEE Transactions on Communications*, 53(1):74–83.
- Mueller-Weinfurter, S. H. (2002). Coding Approaches for Multiple Antenna Transmission in Fast Fading and OFDM. *IEEE Transactions on Signal Processing*, 50(10):2442–2450.
- Proakis, J. G. (2000). *Digital Communications*. McGraw-Hill, Boston.
- Raleigh, G. G. and Cioffi, J. M. (1998). Spatio-Temporal Coding for Wireless Communication. *IEEE Transactions on Communications*, 46(3):357–366.
- Raleigh, G. G. and Jones, V. K. (1999). Multivariate Modulation and Coding for Wireless Communication. *IEEE Journal on Selected Areas in Communications*, 17(5):851–866.
- Schreckenbach, F. and Bauch, G. (2006). Bit-Interleaved Coded Irregular Modulation. *European Transactions on Telecommunications*, 17(2):269–282.
- Wong, C. Y., Cheng, R. S., Letaief, K. B., and Murch, R. D. (1999). Multiuser OFDM with Adaptive Subcarrier, Bit, and Power Allocation. *IEEE Journal on Selected Areas in Communications*, 17(10):1747–1758.
- Zheng, L. and Tse, D. N. T. (2003). Diversity and Multiplexing: A Fundamental Tradeoff in Multiple-Antenna Channels. *IEEE Transactions on Information Theory*, 49(5):1073–1096.
- Zhou, Z., Vucetic, B., Dohler, M., and Li, Y. (2005). MIMO Systems with Adaptive Modulation. *IEEE Transactions on Vehicular Technology*, 54(5):1073–1096.